ACS OMEGA

Article

Cite This: ACS Omega 2019, 4, 14765−14771

http://pubs.acs.org/journal/acsodf

Signal Enhancement of Silicon Nanowire Field-Effect Transistor Immunosensors by RNA Aptamer

Cao-An Vu,[†] Wen-Pin Hu,[‡] Yuh-Shyong Yang,[§] Hardy Wai-Hong Chan,[∥] and Wen-Yih Chen*[,†]

[†]Department of Chemical and Materials Engineering, National Central University, Jhongli 320, Taiwan

[‡]Department of Biomedical Informatics, Asia University, Taichung 413, Taiwan

[§]Institute of Biological Science and Technology, National Chiao Tung University, Hsinchu 300, Taiwan

[∥]Helios Bioelectronics Inc., Hsinchu 30261, Taiwan

ABSTRACT: Silicon nanowire field-effect transistors (SiNW-FETs) have been demonstrated as a highly sensitive platform for label-free detection of a variety of biological and chemical entities. However, detecting signal from immunoassays by nano-FETs is severely hindered by the distribution of different charged groups of targeted entities, their binding orientation, and distances to the surface of the FET. Aptamers have been widely applied as a recognition element for plentiful biosensors because of small molecular sizes and moderate to high specific binding affinity with different types of molecules. In this study, we propose an effective approach to enhance the electrical responses of both direct (6×-histidine) and sandwich (amyloid β 1−42) immunoassays in SiNW-FETs with R18, a highly negative charged RNA aptamer against rabbit immunoglobulin G (IgG). Empirical results presented that the immunosensors targeted with R18 expressed a significantly stabilized and amplified signal compared to the ones without this aptamer. The research outcome provides applicability of the highly negative charged aptamer as a bioamplifier for immunoassays by FETs.

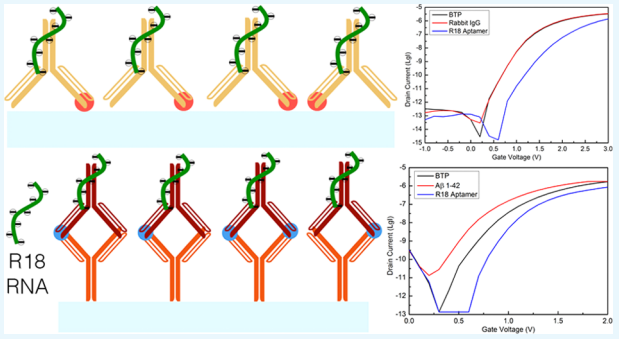

1. INTRODUCTION

Since being invented by Lieber's group in 2001,[1] silicon nanowire field-effect transistor (SiNW-FET) sensors have received particular interests because of their high sensitivity for label-free and real-time detection.[1,2] In fact, ultrasensitive SiNW-FET sensors have been successfully employed for the real-time and label-free detection of proteins,[1−4] nucleic acids,[5−7] viruses,[8,9] and different targeted substances.[1,10−16] Moreover, in comparison with other nanostructure-based sensors, the SiNW-FET sensors have more commercial potential due to their feasibility for mass production in semiconductor industry, especially by the so-called top−down process.[3] However, applying FET nanosensors in clinical trials to detect biomolecules is severely hindered by the ionic screening effect, also known as Debye screening, caused by the high ionic strength of physiological environment (>100 mM).[17] Thus, there are many methods to subdue their detrimental effects on bio-FETs such as performing detection in diluted solutions with low ionic strength[2,4−7,18] and/or employing small molecules as bioreceptors (antibody fragment,[4,18] DNA aptamer,[19] RNA aptamer[20]). Gao et al. revealed another approach to overcome this obstacle by modifying SiNW surface with poly(ethylene glycol) (PEG) to expand the detectable region for biosensing prostate-specific antigen in 150 mM phosphate buffer (PB).[21] To elucidate factors influencing the detection sensitivity of SiNW-FET biosensors via screening effect, while Zhang and co-workers announced that this variable is strongly dependent on the distance between the negatively charge layers of DNA and the nanowire surface,[7] De Vico et al., using theoretical simulation, went a step further to demonstrate that the distribution of various charged groups (positive and negative) throughout protein and their distances to the sensing surface are both determinants.[22] Furthermore, different binding orientations also contribute to dissimilar recorded signal of an immunoassay due to the bulky size and stearic structure of proteins. Nevertheless, to date, there are insufficient data to completely unveil the mystery. Hence, a solution is necessary to overcome these limitations for the detection of protein by FETs in clinical settings, which is the ultimate goal of profuse biomedical applications.[23]

Aptamers, single-stranded oligonucleotides that can be selected from an in vitro process referred to as systematic evolution of ligands by exponential enrichment (SELEX), are capable of binding with numerous molecules with high affinity and specificity.[24] Improvement of the SELEX technique during recent years has also resulted in the development of diverse aptamers that can specifically target immunoresponses.[24] Aptamers have received exhaustive attention for immunoassay because of several advantages. First, it is easy to generate

Received: May 2, 2019
Accepted: July 11, 2019
Published: September 6, 2019

DOI: 10.1021/acsomega.9b01264
ACS Omega 2019, 4, 14765−14771

functional aptamers from the reversible production of the aptamer−target complex[24] or chemical synthesis of sequential phosphoramidite.[25] Second, bioactivity of aptamers is stable over a wide range of thermal conditions.[25] Third, the aptamer−protein binding may favorably be detected by FET even with the screening effect of Debye length regarding to its comparatively small size.[25] More importantly, aptamers with highly negative charged density possibly suppress the effectiveness of various charge groups in proteins and consequently enhance the signal of the FET-based immunosensors. We also propose this hypothesis as a solution for the aforementioned issues by taking advantage of the highly negative charged aptamer as an amplifier for immunoassay in nano-FETs.

In our study, R18, an RNA aptamer recognizing rabbit immunoglobulin G (IgG) with high affinity and specificity,[26] was utilized as an amplifier for nano-FET-based immunosensors. We chose 6×-histidine with its respective rabbit IgGs for direct immunoassay as well as amyloid β 1−42 (Aβ 1−42) with mouse-capturing (IgG1) and rabbit-detection (IgG) antibody for a sandwich type immunoassay. The former is applied in protein engineering such as studies of protein−protein and protein−DNA interactions[27] and protein purification,[28] whereas the latter, a peptide with 42 amino acids, is ubiquitous in the brain cortex of patients with Alzheimer's disease (AD).[29] Amplifying the immunoassay signal of Aβ 1−42 potentially lowers its limit of detection and limit of quantification, leading to a promising vista for the preclinical detection of this biomarker in the early-stage diagnosis of AD, where enzyme-linked immunosorbent assay, the current clinical method, is ineffective due to its extremely low concentration in human blood.[30,31]

2. MATERIALS AND METHODS

2.1. Materials. (3-Aminopropyl)triethoxysilane (APTES), glutaraldehyde, bis-Tris propane (BTP), sodium cyanoborohydride ($NaBH_3CN$), Tris(hydroxymethyl)aminomethane (Tris), and hydrochloric acid (HCl) were delivered by Sigma-Aldrich. Ethanol (99%) was ordered from Echo Chemical Co., Ltd and chemical for photoresist layer removal (EKC 830, component: 2-(2-aminoethoxy)ethanol and *N*-methyl-2-pyrrolydone) was from DuPont. Two peptides (6×-histidine: HHH HHH, Aβ 1−42: DAE FRH DSG YEV HHQ KLV FFA EDV GSN KGA IIG LMV GGV VIA) and their specific antibodies (mouse antibody: isotype IgG1, rabbit antibody: isotype IgG) were supplied by Abcam plc. (U.K.). 10 mM Tris, 10 mM and 150 mM BTP buffers were all prepared in deionized water and adjusted to pH of 7.4 by HCl. The other chemicals for this research were of reagent grade.

R18 aptamer (74-mer RNA sequence: 5′-GGGAG AAUUC CGACC AGAAG UUCGA UACGC CGUGG GGUGA CGUUG GCUAC CCUUU CCUCU CUCCU CCUUC UUCU-3′),[26] which can distinguish rabbit IgG, was synthesized in our laboratory by polymerase chain reaction and RNA transcription from its complementary DNA (cDNA). The former was carried out by primers and cDNA template acquired through MDBio within DreamTaq DNA Polymerase and DreamTaq Buffer supplied by ThermoScientific, the latter was implemented by T7 RiboMAX Express Large Scale RNA Production System from Promega.

2.2. Apparatuses and SiNW-FET Characteristics. The SiNW-FET in this study, fabricated by National Nano Device Laboratory of National Chiao Tung University (Hsinchu, Taiwan), was also used in our previous works.[6,32,33] Length and width of each nanowire channel on the n-type device are 2 μm and 80 nm, respectively. Keithley 2636 Dual-channel System Source Meter Instrument and a probe station with a chamber (Everbeing) were employed to measure the current−voltage ($I-V$) characteristics of the SiNW-FET sensor. A programming syringe pump (KD Scientific) and a microfluidic system possessing channel dimension of 5 × 0.5 × 0.1 mm^3 were integrated with the fabricated sensor to transport the liquids continuously through the nanowires at a flow rate of 5 mL/h. Before performing biomolecular interactions with the SiNW-FET biochip to analyze its immunoassay through drain current−gate voltage (I_d-V_g) curve, gauging the current of the fabricated sensor was triplicated after incubating it in 150 mM BTP buffer for 5 min to regulate its signal and establish the baseline to evaluate the electrical properties produced from biorecognition events.

2.3. Immobilization of Biomolecules on SiNW-FET Surface. Initially, the SiNW-FET chips were cleansed to remove the photoresist layer by immersing in EKC 830 at 95 °C for 20 min, followed by 10 min sonication in deionized water and drying with nitrogen for three times. These SiNW-FET chips were then treated with oxygen plasma for 10 min before chemical surface modification with APTES and glutaraldehyde. This stage started with gentle shaking of the chips in a 2% APTES solution (99% ethanol as the solvent) for 30 min on a platform rocker operating at 60 rpm and ambient temperature. Afterward, they were sonicated in 99% ethanol to remove the APTES residues and treated at 120 °C for 10 min. This procedure was completed with glutaraldehyde functionalization by gently shaking the APTES-modified SiNW-FET chip at 60 rpm and room temperature in a container of 2.5% glutaraldehyde in 10 mM BTP for 60 min, followed by sonication in 10 mM BTP for 10 min to remove glutaraldehyde residues. These SiNW-FET chips were finally ready for biomolecular immobilization.

The bioprobes (hexahistidine or mouse anti-A$\beta_{1\text{-}42}$ antibody) were immobilized on the surface of APTES-glutaraldehyde-modified chips by incubating them in sealed Petri dishes at 4 °C overnight with 10 mM BTP solution containing 0.4% $NaBH_3CN$ and either 1 μg/mL hexahistidine or mouse anti-A$\beta_{1\text{-}42}$ IgG1 on the surface. The next day, these chips were initially shaken in 10 mM BTP for 10 min by a platform rocker to remove nonspecific binding on the nanowire surface. Eventually, 0.4% $NaBH_3CN$ in 10 mM Tris was utilized as a blocking buffer for the FET surface by shaking it twice on a platform rocker for 10 min each within the buffer exchange before the final purification by deionized water and desiccation by nitrogen. These immune-SiNW-FET chips were then ready to be installed into the FET system for biosensing measurements.

2.4. Direct and Sandwich Immunoassay by SiNW-FET and Signal Amplification by Aptamer. Enhancement of the signal produced from direct immunoassays of the 6×-histidine peptide immobilized on the sensor surface is illustrated in Figure 1. After installing the SiNW-FET chip in the instrument system and stabilizing the signal of the I_d-V_g curve in the BTP buffer, BTP containing 1 μg/mL anti-hexahistidine rabbit IgG was transported through the nanowire field-effect transistor (NWFET) sensor at a rate of 5 mL/h for 10 min. The I_d-V_g curve was then plotted after a 30 min incubation with this IgG and a 10 min washing with the BTP buffer. Subsequently, R18 aptamer was injected into the SiNW-

DOI: 10.1021/acsomega.9b01264
ACS Omega 2019, 4, 14765−14771

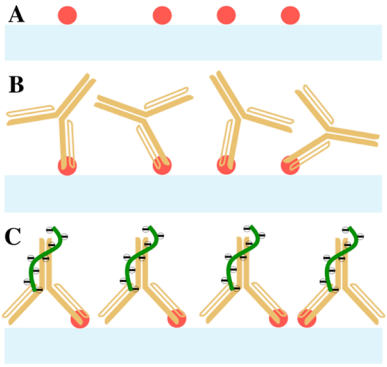

Figure 1. Schematic diagram of the direct immunoassay performed on the SiNW-FET biosensor in this study: (A) 6×-histidine (red dots) was immobilized on the nanowire channel (light blue bar) before transporting (B) its respective rabbit IgG (yellow Y shapes) for immunoassay and (C) R18 RNA aptamer (green curves) for signal enhancement.

FET sensor at similar rate and time used for antibody transportation (Figure 1). The I_d−V_g curve was also measured again after a 30 min incubation and a 10 min washing with the BTP buffer. These procedures were also repeated to enhance the signal begot by sandwich immunoassay with Aβ 1−42. However, an additional phase of injection−incubation−washing with rabbit anti-A$\beta_{1\text{-}42}$ antibody was required between the treatments of Aβ 1−42 and R18 to assure the presence of this RNA aptamer on the sensor surface (Figure 2).

3. RESULTS AND DISCUSSION

In a SiNW-FET system, the receptors are immobilized on the nanowire surface to detect the analytes with highly specific binding affinity. The recognition of the targets by the probes changes surface potential and modulates the channel conductance, which are recorded and further processed by the electrical measurement system. Since our chips are n-type FETs, accumulation of charge carriers by capturing positive charged molecules of the anchored bioreceptors increases the conductance and depletion of charge carriers due to the binding of negative charged molecules with immobilized recognition elements results in the reduction of conductance. We used 150 mM BTP buffer and pH 7.4 for our experiments, which are not only identical with the binding conditions of R18 and rabbit IgG in the SELEX process[26] but also approximately analogous to the physiological condition. In this study, the electrical data were quantitatively analyzed by selecting the drain current (I_d) at 10^{-9} A (LgI = −9 in Figures 3 and 4) and calculating the change of gate voltage (ΔV) initiated by the formation of biocomplexes (hexahistidine-IgG, hexahistidine-IgG-R18, IgG1-Aβ_{1-42}, IgG1-Aβ_{1-42}-IgG-R18) from the formula

$$\Delta V = V_{d1} - V_{d0} \quad (1)$$

where V_{d1} is the gate voltage for the electrical response actuated after the binding of the biological entities (Aβ 1−42 to mouse anti-A$\beta_{1\text{-}42}$ IgG1; rabbit anti-hexahistidine IgG to 6×-His, R18 RNA aptamer to two kinds of rabbit antibodies) at I_d = 10^{-9} A (LgI = −9) and V_{d0} is the gate voltage for the electric response generated by the 150 mM BTP buffer (baseline) at I_d = 10^{-9} A (LgI = −9). Statistical data for each experiment were collected from fifteen devices of at least three distinctive biochips (five devices per chip) manufactured by different batch productions.

3.1. Immunoassay of Hexahistidine by SiNW-FET and Signal Stabilization by R18. Electric currents of the SiNW-FET sensors for the anchored 6×-histidine peptide and rabbit IgG complex on the sensing surface are characterized in Figure 1. Evidently, there are three dissimilar trends in the signal produced by the sensors after injection of rabbit IgG. On the one hand, the lower drain current (ΔV = 320 ± 203 mV in the inset of Figure 3A) after the peptide−IgG complex formation is attributed to a depletion of charge carriers on the modified surface, suggesting that the net charge of the antibody is negative at pH 7.4. On the other hand, a higher drain current in Figure 3B (inset: ΔV = −237 ± 114 mV) indicates a positive net charge of the antibody at pH 7.4, which resulted in an accumulation of charge carriers on the fabricated surface. In addition, there is also almost unchanged electrical signal before and after transportation of the rabbit anti-hexahistidine antibody to the immobilized peptide (Figure 3C and its insets: ΔV = 1 ± 49 mV). Except the variations from chip production and surface modification process, the distance between the antibody and the silicon surface is also a key factor, which is very difficult to uniformly control in this direct immunoassay. Indeed, distinctive charged groups distributed throughout the IgG molecules differently affect the sensing surface due to their various distances to the nanowire, which are managed by individual binding orientations of these antibodies, and the screening effect. Besides, the signal-to-noise

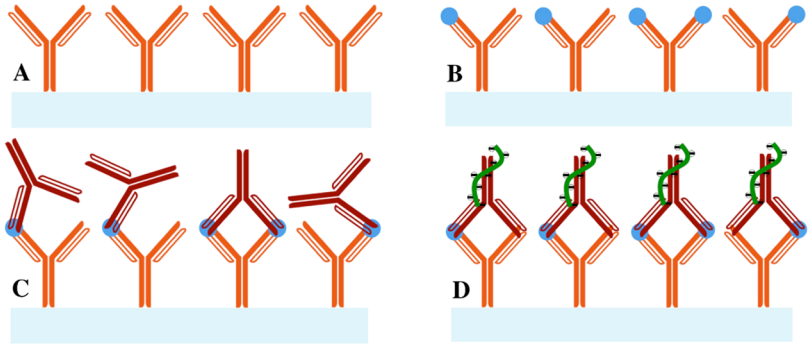

Figure 2. Schematic diagram of the sandwich immunoassay performed on the SiNW-FET biosensor in this study: (A) mouse IgG1 (orange Y shapes) was immobilized on the nanowire channel (light blue bar) to detect (B) Aβ 1−42 peptide (blue dots) through its amino acids 1−17. The immunosensors were then exposed to (C) rabbit IgG (red Y shapes), which reacts with amino acids 33−42 of Aβ 1−42 peptide, followed by (D) R18 RNA aptamer (green curves) for signal enhancement.

DOI: 10.1021/acsomega.9b01264
ACS Omega 2019, 4, 14765−14771

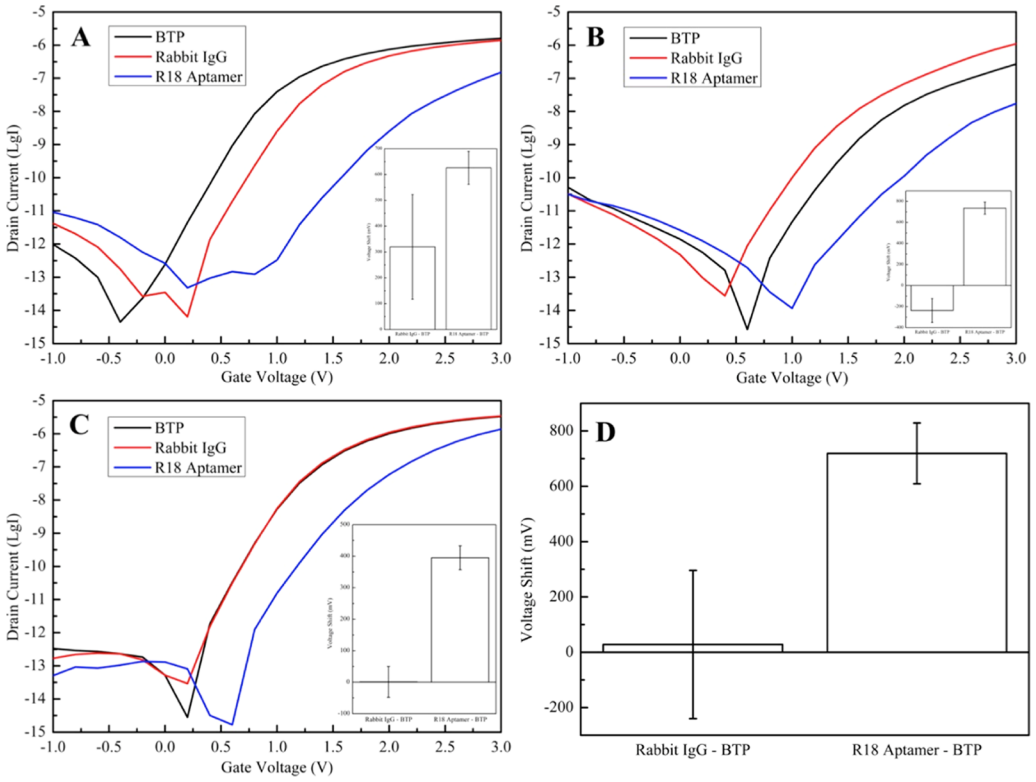

Figure 3. Electrical signal of the SiNW-FET chip immobilized with 6×-histidine peptide after incubation of nanowire channels with 150 mM BTP buffer (black curve) and 1 μg/mL rabbit anti-6×-His antibody (IgG) in 150 mM BTP buffer (red curve), followed by ~6 μg/mL R18 RNA in 150 mM BTP buffer (blue curve). The conductance significantly reduces with the presence of R18, although it can (A) decrease, (B) increase, or (C) even remain mostly unchanged after IgG detection. Insets are their corresponding statistical data as ΔV = mean ± standard deviation (n = 5) after detecting rabbit IgG ($\Delta V_{\text{IgG-BTP}}$) and R18 RNA ($\Delta V_{\text{R18-BTP}}$) (A: $\Delta V_{\text{IgG-BTP}}$ = 320 ± 203 mV, $\Delta V_{\text{R18-BTP}}$ = 626 ± 64 mV; B: $\Delta V_{\text{IgG-BTP}}$ = −237 ± 114 mV, $\Delta V_{\text{R18-BTP}}$ = 736 ± 58 mV; C: $\Delta V_{\text{IgG-BTP}}$ = 1 ± 49 mV, $\Delta V_{\text{R18-BTP}}$ = 395 ± 38 mV). (D) Total statistical data for signal amplification of this direct immunoassay by the aptamer as ΔV = mean ± standard deviation (n = 15) ($\Delta V_{\text{IgG-BTP}}$ = 28 ± 268 mV, $\Delta V_{\text{R18-BTP}}$ = 719 ± 110 mV).

ratio possibly contributes to the unsteady electrical signal of the immunoassay by nano-FETs. In summary, it is unable to detect the signal produced by the immunoassay of 6×-histidine peptide and its corresponding rabbit IgG from irregular electrical response of SiNW-FET due to the screening effect and binding orientation of the antibody (ΔV = 28 ± 268 mV in Figure 3D).

The applicability of the synthesized R18 RNA aptamer for the signal amplification of direct immunoassay with 6×-histidine on the SiNW-FET sensor was investigated at final concentration of approximately 6 μg/mL. Obviously, the R18 aptamer could bind with the IgG of the rabbit anti-hexahistidine antibody and activate apparent conductance changes in the FET-based nanosensors. Notably, the current always considerably declined with the R18 aptamer regardless to its unsteadiness induced by the rabbit IgG (Figure 3A−C). According to the calculated result by eq 1, the formed aptamer−antibody−peptide complex in this experiment provoked a different potential from the baseline ΔV = 719 ± 110 mV (Figure 3D), which not only vanished the discrepancy but also amplified the signal of the 6×-His immunoassay in SiNW-FET. A minor potential change ΔV = 36 ± 14 mV (data are not illustrated) obtained after incubating R18 on the modified surface without rabbit IgG evinces that this RNA aptamer was not recognized by histidine chains, eliminating suspicion about the nonspecific binding contributing to the enhanced outcome. High specificity between R18 and rabbit IgG is therefore vital for this proof of concept.

3.2. Signal Stabilization by R18 for Amyloid β 1−42 Detection by SiNW-FET. Motivated by the success of the R18 aptamer for the direct immunoassay of 6×-histidine, we exploited it for the immunoassay of human Aβ 1−42, a longer peptide with 42 amino acids, in which this peptide was detected by a mouse antibody corresponding to its amino acids 1−17 immobilized on the surface of the SiNW-FET. Figure 4 describes the recorded signal from the immunosensors before and after exposure to Aβ 1−42, the rabbit IgG recognizing amino acids 33−42 of Aβ 1−42, and the aptamer. They shuffle to both left (rise up with ΔV = −198 ± 7 mV, Figure 4B) and right (fall down with ΔV = 175 ± 17 mV, Figure 4A) sides of the baseline, indicating an inconsistency in the current trends caused by Aβ 1−42. Thus, the potency of the R18 aptamer in stabilizing the signal was examined through the assistance of the rabbit antibody mentioned above. Theoretically, its epitope is able to detect amino acids 33−42 of Aβ 1−42, on one hand, and its constant region is capable of binding with the R18 aptamer, on the other hand.[26] Apparently, these binding reactions could activate current changes in the sensor. Similar to the acquisition from the direct immunoassay of 6×-His, a sharply weakened current of the sensors is always observed after contacting with the RNA aptamer (ΔV = 208 ± 31 mV from the baseline in Figure 4C). Additionally, inspecting the relation of nonspecific binding between rabbit IgG and R18 to the sensing channels by incubating sensors in them without detecting Aβ 1−42 resulted in ΔV = 64 ± 13 mV (Figure 4D), referring to the insignificant contribution of the nonspecific

DOI: 10.1021/acsomega.9b01264
ACS Omega 2019, 4, 14765−14771

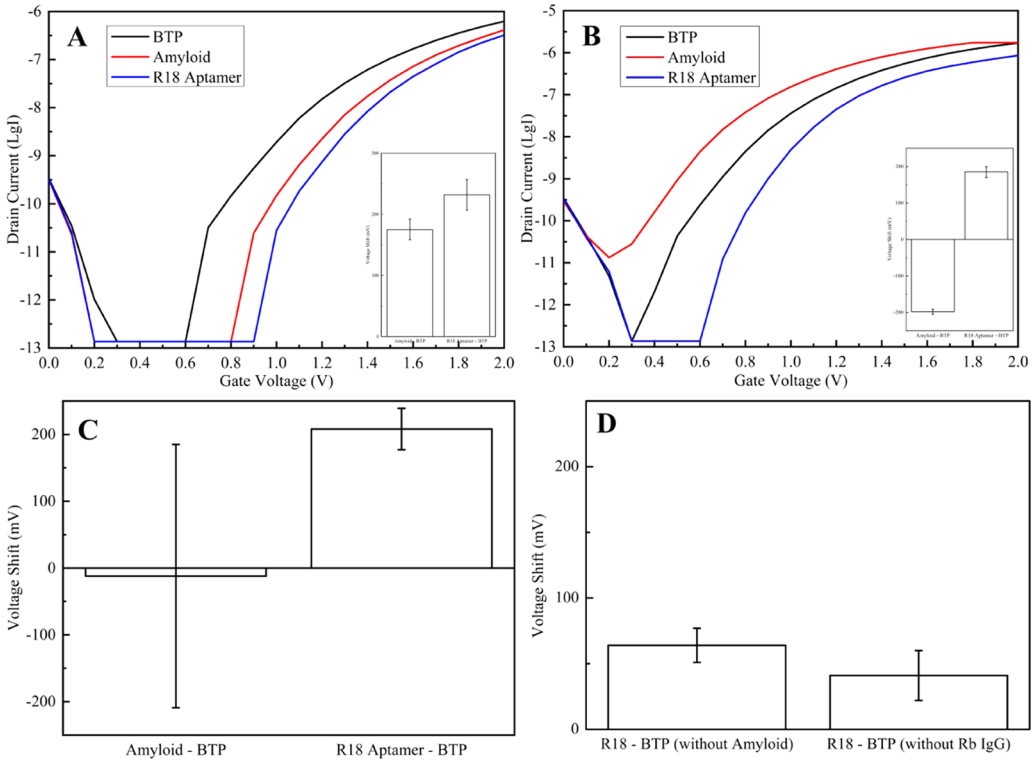

Figure 4. Electrical signals of the SiNW-FET chip immobilized with mouse anti-A$\beta_{1\text{-}42}$ antibody (IgG1) after exposing it to 150 mM BTP (black curve) and 1 μg/mL Aβ 1−42 in 150 mM BTP buffer (red curve), followed by 1 μg/mL rabbit anti-A$\beta_{1\text{-}42}$ antibody (IgG) and ∼3 μg/mL R18 RNA in 150 mM BTP buffer (blue curve). The conductance significantly reduces with the presence of R18, although it can decrease (A) or increase (B) after detecting Aβ 1−42 peptide. Insets are their corresponding statistical data as ΔV = mean ± standard deviation (n = 5) after recognizing Aβ 1−42 ($\Delta V_{A\beta\text{-BTP}}$) and R18 RNA ($\Delta V_{R18\text{-BTP}}$) (A: $\Delta V_{A\beta\text{-BTP}}$ = 175 ± 17 mV, $\Delta V_{R18\text{-BTP}}$ = 232 ± 25 mV; B: $\Delta V_{A\beta\text{-BTP}}$ = −198 ± 7 mV, $\Delta V_{R18\text{-BTP}}$ = 185 ± 15 mV). Total statistical data for signal amplification of this sandwich immunoassay by the aptamer (C, n = 10: $\Delta V_{A\beta\text{-BTP}}$ = −12 ± 197 mV, $\Delta V_{R18\text{-BTP}}$ = 208 ± 31 mV) and its control experiments (D, n = 5) after injecting R18 without incubation of either Aβ 1−42 ($\Delta V_{R18\text{-BTP}}$ = 64 ± 13 mV) or rabbit anti-A$\beta_{1\text{-}42}$ IgG ($\Delta V_{R18\text{-BTP}}$ = 41 ± 19 mV).

binding between the fabricated surface and the rabbit IgG and/or R18 aptamer to signal enhancement. Finally, the sensors were also exposed to R18 without the presence of the rabbit antibody on their surfaces after capturing the peptide and generated a trivial voltage shift (ΔV = 41 ± 19 mV from the baseline in Figure 2D), which is supposedly due to the noise of the signal. It establishes the fact that R18 is only recognized by the rabbit IgG and undetected by any peptide. The rabbit IgG (for instance, corresponding to amino acids 33−42 of Aβ 1−42 in this experiment) is hence indispensable and plays a crucial part in stabilizing and amplifying the signal changes actuated by Aβ 1−42. This immunoassay accordingly becomes a so-calledsandwich immunoassay.

3.3. Aptamer—Pivotal Appearance and Inevitable Involvement in Future Prospects of Immuno-FET Nanosensors. In fact, the R18 aptamer is not only a molecule that specifically binds with the rabbit IgG but also an RNA sequence that carries copious amount of negatively charged phosphate group in its sequence. For those reasons, the R18 aptamer feasibly binds to the rabbit IgG antibody on the sensor surface and suppresses the effectiveness of different charged groups distributed throughout the antibody structure as well as improves the signal-to-noise ratio of the SiNW-FET to result in a significant reduction in conductance and achieve signal stabilization and amplification of the immunoassays on the FET-based nanosensors. Remarkably, in comparison with a secondary antibody, the R18 aptamer is not only more compact but also recognizes rabbit IgG with at least two target binding sites (residues G20, U21, and G24 in stem 1 and residues U38, C41, G45, and C47 in loop 2 of its secondary structure) and almost entirely covers rabbit IgG.[26] As a result, their binding interaction almost takes place within the same Debye length of the antibody, and the negative charges carried by the R18 aptamer are not severely weakened by the screening effect, suggesting that electrical responses to the silicon surface are detectable in the measurement. Additionally, we also suppose that the R18 binding to rabbit IgG can trigger intermolecular repulsive forces to modulate the intermolecular layer of the peptide−antibody complex, therefore a positive and steady electrical signal is distinguishable after using the R18 aptamer. Generally, signal enhancement is mainly contributed by this highly negative charged R18 aptamer. Relevant to vigorous negative charged oligonucleotides on nano-FETs, Gao et al., in an effort to improve the signal-to-noise ratio of nanowire devices, used a rolling circle amplification (RCA) reaction to yield a long single-stranded DNA for achieving ultrasensitive hepatitis B virus (HBV) DNA detection.[34] Binding of prolific repeated sequences of RCA products created significantly amplified signal from abundant negative charges on the nanowire surface.[34] These features indicate that the designed solution is feasible and provides excellent efficiency for signal enhancement on the SiNW-FET sensors. Compared to previous publications on similar topics,[2,4−7,17,18] this method directly accomplished the biodetection in such a high ionic strength condition of up to 150 mM BTP without dissecting the antibody for antigen-

DOI: 10.1021/acsomega.9b01264
ACS Omega 2019, 4, 14765−14771

binding fragments or expanding sensible area through desalting action. It is consequently more precise, convenient, time-saving, and particularly advantageous for assays in which analyte dilution is inappropriate and must be operated in serum samples with a diversity of proteins. For instance, diluting plasma samples of AD markers is seemingly impractical due to its ultralow concentration in human blood and cerebrospinal fluid (<1 pM).[35] Moreover, this sensing strategy is appropriate not only for direct immunoassay, which includes immobilizing antigen (target molecule) on the sensor surface and dissolving antibody (receptor) in the solution, but also sandwich immunoassay, which contains antigen (target molecule) between two layers of antibodies (capture and detection antibody), on the SiNWFET sensors. There are multiple options of aptamer and capture and detection antibody for both immunoassay models provided that the association between the detection antibody and the aptamer is validated. For example, an 84-mer DNA aptamer specifying mouse IgG[36] may equivalently effectuate the signal of SiNWFET immunosensors as R18 did. In summary, we conclude that the antibody−aptamer coalition is an exclusive approach and irresistible for application of the SiNW-FET sensors to stabilize and enhance the signal detected from both direct and sandwich immunoassays.

4. CONCLUSIONS

In SiNW-FET-based biosensors, since the screening effect imposed by the ionic strength of physiological environment has detrimental consequence on their sensitivity, signal recognition of immunoassay is severely hindered by the individual distance of several charged group distributed throughout the protein structure to the sensing surface and the binding orientation of the analytes with the bioreceptors. Herein, we demonstrate that specific binding of aptamer−antibody could steadily produce a substantial conductance change and aptamer is practically applied as a signal amplifier for the SiNW-FET immunosensors because of its high charge density and relatively small molecular framework. The suggested solution, being reported for the first time, is proved to be successful for both direct (6×-histidine) and sandwich (Aβ 1−42) immunoassays with rabbit IgG antibody. The strategy offered in this study is potentially applicable for the detection of other macromolecules with different charged group in vitro and in vivo by nano-FETs.

AUTHOR INFORMATION

Corresponding Author

*E-mail: wychen@ncu.edu.tw. Tel: + 886-3-422-7151#34222. Fax: +886-3-422-5258.

ORCID

Cao-An Vu: 0000-0001-7646-1039

Wen-Pin Hu: 0000-0003-1826-7689

Yuh-Shyong Yang: 0000-0003-0177-473X

Notes

The authors declare no competing financial interest.

ACKNOWLEDGMENTS

Financial support from the Ministry of Science and Technology (MOST), Taiwan (Grant no. 106-2622-8-009-012-TM and Grant no. 107-2622-8-009-010-TM) is greatly appreciated.

REFERENCES

(1) Cui, Y.; Wei, Q.; Park, H.; Lieber, C. M. Nanowire Nanosensors for Highly Sensitive and Selective Detection of Biological and Chemical Species. *Science* **2001**, *293*, 1289−1292.

(2) Chua, J. H.; Chee, R. -E.; Agarwal, A.; Wong, S. M.; Zhang, G.-J. Label-Free Electrical Detection of Cardiac Biomarker with Complementary Metal-Oxide Semiconductor-Compatible Silicon Nanowire Sensor Arrays. *Anal. Chem.* **2009**, *81*, 6266−6271.

(3) Stern, E.; Klemic, J. F.; Routenberg, D. A.; Wyrembak, P. N.; Turner-Evans, D. B.; Hamilton, A. D.; LaVan, D. A.; Fahmy, T. M.; Reed, M. A. Label-free Immunodetection with CMOS-compatible Semiconducting Nanowires. *Nature* **2007**, *445*, 519−522.

(4) Cheng, S.; Hotani, K.; Hideshima, S.; Kuroiwa, S.; Nakanishi, T.; Hashimoto, M.; Mori, Y.; Osaka, T. Field Effect Transistor Biosensor Using Antigen Binding Fragment for Detecting Tumor Marker in Human Serum. *Materials* **2014**, *7*, 2490−2500.

(5) Gao, Z.; Agarwal, A.; Trigg, A. D.; Singh, N.; Fang, C.; Tung, C.-H.; Fan, Y.; Budhharaju, K. D.; Kong, J. Silicon Nanowire Arrays for Label-Free Detection of DNA. *Anal. Chem.* **2007**, *79*, 3291−3297.

(6) Chen, W.-Y.; Chen, H.-C.; Yang, Y.-S.; Huang, C.-J.; Chan, H. W.-H.; Hu, W.-P. Improved DNA Detection by Utilizing Electrically Neutral DNA Probe in Field-effect Transistor Measurements as Evidenced by Surface Plasmon Resonance Imaging. *Biosens. Bioelectron.* **2013**, *41*, 795−801.

(7) Zhang, G.-J.; Zhang, G.; Chua, J. H.; Chee, R.-E.; Wong, E. H.; Agarwal, A.; Buddharaju, K. D.; Singh, N.; Gao, Z.; Balasubramanian, N. DNA Sensing by Silicon Nanowire: Charge Layer Distance Dependence. *Nano Lett.* **2008**, *8*, 1066−1070.

(8) Zhang, G.-J.; Zhang, L.; Huang, M. J.; Luo, Z. H. H.; Tay, G. K. I.; Lim, E.-J. A.; Kang, T. G.; Chen, Y. Silicon Nanowire Biosensor for Highly Sensitive and Rapid Detection of Dengue Virus. *Sens. Actuators, B* **2010**, *146*, 138−144.

(9) Hideshima, S.; Hinou, H.; Ebihara, D.; Sato, R.; Kuroiwa, S.; Nakanishi, T.; Nishimura, S.-I.; Osaka, T. Attomolar Detection of Influenza A Virus Hemagglutinin Human H1 and Avian H5 Using Glycan-Blotted Field Effect Transistor Biosensor. *Anal. Chem.* **2013**, *85*, 5641−5644.

(10) Field, C. R.; In, H. J.; Begue, N. J.; Pehrsson, P. E. Vapor Detection Performance of Vertically Aligned, Ordered Arrays of Silicon Nanowires with a Porous Electrode. *Anal. Chem.* **2011**, *83*, 4724−4728.

(11) Zhang, G.-J.; Huang, M. J.; Ang, J. J.; Yao, Q.; Ning, Y. Label-Free Detection of Carbohydrate−Protein Interactions Using Nanoscale Field-Effect Transistor Biosensors. *Anal. Chem.* **2013**, *85*, 4392−4397.

(12) Chen, H.-C.; Qiu, J.-T.; Yang, F.-L.; Liu, Y.-C.; Chen, M.-C.; Tsai, R.-Y.; Yang, H.-W.; Lin, C.-Y.; Lin, C.-C.; Wu, T.-S.; Tu, W.-M.; Xiao, M.-C.; Ho, C.-H.; Huang, C.-C.; Lai, C.-S.; Hua, M.-Y. Magnetic-Composite-Modified Polycrystalline Silicon Nanowire Field-Effect Transistor for Vascular Endothelial Growth Factor Detection and Cancer Diagnosis. *Anal. Chem.* **2014**, *86*, 9443−9450.

(13) Chen, Y.; Wang, X.; Hong, M.; Erramilli, S.; Mohanty, P. Surface-modified Silicon Nano-channel for Urea Sensing. *Sens. Actuators, B* **2008**, *133*, 593−598.

(14) Chang, K. S.; Chen, C. C.; Sheu, J. T.; Li, Y.-K. Detection of An Uncharged Steroid with A Silicon Nanowire Field-effect Transistor. *Sens. Actuators, B* **2009**, *138*, 148−153.

(15) Komarova, N. V.; Andrianova, M. S.; Gubanova, O. V.; Kuznetsov, E. V.; Kuznetsov, A. E. Development of a novel enzymatic biosensor based on an ion-selective field effect transistor for the detection of explosives. *Sens. Actuators, B* **2015**, *221*, 1017−1026.

(16) Manga, Y. B.; Ko, F.-H.; Yang, Y.-S.; Hung, J.-Y.; Yang, W.-L.; Huang, H.-M.; Wu, C.-C. Ultra-fast and Sensitive Silicon Nanobelt Field-effect Transistor for High-throughput Screening of Alpha-fetoprotein. *Sens. Actuators, B* **2018**, *256*, 1114−1121.

(17) Stern, E.; Wagner, R.; Sigworth, F. J.; Breaker, R.; Fahmy, T. M.; Reed, M. A. Importance of the Debye Screening Length on Nanowire Field Effect Transistor Sensors. *Nano Lett.* **2007**, *7*, 3405−3409.

DOI: 10.1021/acsomega.9b01264
ACS Omega 2019, 4, 14765−14771

(18) Elnathan, R.; Kwiat, M.; Pevzner, A.; Engel, Y.; Burstein, L.; Khatchtourints, A.; Lichtenstein, A.; Kantaev, R.; Patolsky, F. Biorecognition Layer Engineering: Overcoming Screening Limitations of Nanowire-based FET Devices. *Nano Lett.* **2012**, *12*, 5245−5254.
(19) Kim, K. S.; Lee, H.-S.; Yang, J.-A.; Jo, M.-H.; Hahn, S. K. The Fabrication, Characterization and Application of Aptamer-functionalized Si-nanowire FET Biosensors. *Nanotechnology* **2009**, *20*, No. 235501.
(20) Lee, H.-S.; Kim, K. S.; Kim, C.-J.; Hahn, S. K.; Jo, M.-H. Electrical Detection of VEGFs for Cancer Diagnoses Using Anti-vascular Endotherial Growth Factor Aptamer-modified Si Nanowire FETs. *Biosens. Bioelectron.* **2009**, *24*, 1801−1805.
(21) Gao, N.; Zhou, W.; Jiang, X.; Hong, G.; Fu, T.-M.; Lieber, C. M. General Strategy for Biodetection in High Ionic Strength Solutions Using Transistor-based Nanoelectronic Sensors. *Nano Lett.* **2015**, *15*, 2143−2148.
(22) De Vico, L.; Iversen, L.; Sorensen, M. H.; Brandbyge, M.; Nygard, J.; Martinez, K. L.; Jensen, J. H. Predicting and Rationalizing the Effect of Surface Charge Distribution and Orientation on Nanowire Based FET Bio-sensors. *Nanoscale* **2011**, *3*, 2635−2640.
(23) Stern, E.; Vacic, A.; Rajan, N. K.; Criscione, J. M.; Park, J.; Ilic, B. R.; Mooney, D. J.; Reed, M. A.; Fahmy, T. M. Label-free Biomarker Detection from Whole Blood. *Nat. Nanotechnol.* **2010**, *5*, 138−142.
(24) Hu, P.-P. Recent Advances in Aptamers Targeting Immune System. *Inflammation* **2017**, *40*, 295−302.
(25) Khung, Y. L.; Narducci, D. Synergizing Nucleic Acid Aptamers with 1-dimensional Nanostructures as Label-free Field-effect Transistor Biosensors. *Biosens. Bioelectron.* **2013**, *50*, 278−293.
(26) Yoshida, Y.; Sakai, N.; Masuda, H.; Furuichi, M.; Nishikawa, F.; Nishikawa, S.; Mizuno, H.; Waga, I. Rabbit Antibody Detection with RNA Aptamers. *Anal. Biochem.* **2008**, *375*, 217−222.
(27) Wegner, G. J.; Lee, H. J.; Marriott, G.; Corn, R. M. Fabrication of Histidine-tagged Fusion Protein Arrays for Surface Plasmon Resonance Imaging Studies of Protein−Protein and Protein−DNA Interactions. *Anal. Chem.* **2003**, *75*, 4740−4746.
(28) Bornhorst, J. A.; Falke, J. J. Purification of Proteins Using Polyhistidine Affinity Tags. *Methods Enzymol.* **2000**, *326*, 245−254.
(29) Hardy, J. A.; Higgins, G. A. Alzheimer's Disease: The Amyloid Cascade Hypothesis. *Science* **1992**, *256*, 184−185.
(30) Sehlin, D.; Sollvander, S.; Paulie, S.; Brundin, R.; Ingelsson, M.; Lannfelt, L.; Pettersson, F. E.; Englund, H. Interference from Heterophilic Antibodies in Amyloid-β Oligomer ELISAs. *J. Alzheimer's Dis.* **2010**, *21*, 1295−1301.
(31) Nostrand, W. E. V.; Wagner, S. L.; Shankle, W. R.; Farrow, J. S.; Dick, M.; Rozemuller, J. M.; Kuiper, M. A.; Wolster, E. C.; Zimmerman, J.; Cotman, C. W.; Cunningham, D. D. Decreased Levels of Soluble Amyloid-β Protein Precursor in Cerebrospinal Fluid of Live Alzheimer Disease Patients. *Proc. Natl. Acad. Sci. U.S.A.* **1992**, *89*, 2551−2555.
(32) Lin, H.-C.; Lee, M.-H.; Su, C.-J.; Huang, T.-Y.; Lee, C. C.; Yang, Y.-S. A Simple and Low-cost Method to Fabricate TFTs with Poly-Si Nanowire Channel. *IEEE Electron Device Lett.* **2005**, *26*, 643−645.
(33) Huang, Y.-W.; Wu, C.-S.; Chuang, C.-K.; Pang, S.-T.; Pan, T.-M.; Yang, Y.-S.; Ko, F.-H. Real-Time and Label-Free Detection of the Prostate-Specific Antigen in Human Serum by a Polycrystalline Silicon Nanowire Field-Effect Transistor Biosensor. *Anal. Chem.* **2013**, *85*, 7912−7918.
(34) Gao, A.; Zou, N.; Dai, P.; Lu, N.; Li, T.; Wang, Y.; Zhao, J.; Mao, H. Signal-to-Noise Ratio Enhancement of Silicon Nanowires Biosensor with Rolling Circle Amplification. *Nano Lett.* **2013**, *13*, 4123−4130.
(35) Georganopoulou, D. G.; Chang, L.; Nam, J. -M.; Thaxton, C. S.; Mufson, E. J.; Klein, W. L.; Mirkin, C. A. Nanoparticle-based Detection in Cerebral Spinal Fluid of a Soluble Pathogenic Biomarker for Alzheimer's Disease. *Proc. Natl. Acad. Sci. U.S.A.* **2005**, *102*, 2273−2276.
(36) Ma, J.; Wang, M. G.; Mao, A. H.; Zeng, J. Y.; Liu, Y. Q.; Wang, X. Q.; Ma, J.; Tian, Y. J.; Ma, N.; Yang, N.; Wang, L.; Liao, S. Q. Target Replacement Strategy for Selection of DNA Aptamers Against the Fc Region of Mouse IgG. *Genet. Mol. Res.* **2013**, *12*, 1399−1410.

DOI: 10.1021/acsomega.9b01264
ACS Omega 2019, 4, 14765−14771